Optica Applicata, Vol. XLIII, No. 4, 2013
DOI: 10.5277/oa130403

Engineering the optical and mechanical properties exhibited by a titanium dioxide thin film with gold nanoparticles

SAMUEL MORALES-BONILLA[1], CARLOS TORRES-TORRES[1], MARTÍN TREJO-VALDEZ[2*], DAVID TORRES-TORRES[3], GUILLERMO URRIOLAGOITIA-SOSA[1], LUIS-HÉCTOR HERNÁNDEZ-GÓMEZ[1], GUILLERMO URRIOLAGOITIA-CALDERÓN[1]

[1]Sección de Estudios de Posgrado e Investigación, ESIME ZAC, Instituto Politécnico Nacional, México, D.F., 07738, México

[2]ESIQIE, Instituto Politécnico Nacional, México, D.F. 07738, México

[3]Materials Science and Engineering, CIMAV, Unidad Monterrey, Apodaca, N.L., 66600, México

[*]Corresponding author: martin.trejo@laposte.net

Thermo-optic and electrostrictive contributions to the nonlinear refractive index were observed in a titanium dioxide thin film with embedded gold nanoparticles. A sol–gel method was employed for preparing thin solid film samples. The nanosecond nonlinear optical properties and the Young's modulus parameter were changed by shifting the optical absorption band associated with the localized surface plasmon of resonance of the gold nanoparticles with platinum. The third order nonlinear optical phenomena exhibited by the sample were induced by the second harmonic of a Nd-YAG laser with 532 nm wavelength; the nonlinear optical measurements were obtained by monitoring the transmittance and the amplitude modification for the vectorial components of the electric fields in a two-wave interaction. Optical evaluations were confirmed considering a straightforward measurement of the change in the refractive index of the sample when the sample was located in a Michelson interferometer.

Keywords: optical Kerr effect, nonlinear optics, nanomaterials.

1. Introduction

Some of the most astonishing features of advanced optical materials are their fascinating capabilities to interact exhibiting a high selective behavior. Due to the localized surface plasmon of resonance (LSPR) phenomenon, a tuned sharp optical response in engineered nanoparticles (NPs) with metallic nature can be achieved [1]. The LSPR of metallic NPs can be modified by the particle size, particle shape and density of their distribution [2]; besides, the electromagnetic field near and out of the surface of

the NPs is also responsible for the sensibility of the LSPR response [3]. It has been extensively demonstrated that the surrounding of the NPs also gives an important contribution to the LSPR features [4]. Under different environments, similar NPs can present completely opposite nonlinear optical absorptive effects [5]. Diverse optical active Nobel metal NPs have been prepared in TiO_2 substrates by following distinct preparation methods [6–8]. Moreover, the induced intrinsic residual stress seems to be a relevant parameter that can influence basic optical material properties in nanostructures [9]. And therefore, it appears to be evident that the mechanical properties in metallic nanocomposites could be also defined by the modification of the LSPR. In order to get a deeper knowledge of the close relation between mechanical and plasmonic properties, in this work we study the electrostrictive and nonlinear optical response of a TiO_2 thin solid film with Au NPs and Pt. We were able to confirm an important change in the Young's modulus of the sample originated by the shift of the absorption peak of its LSPR.

2. Theory

The dependence on irradiance for the refractive index n is called the optical Kerr effect, and it can be simply described by [10],

$$n = n_0 + n_2 I \tag{1}$$

where n_o is the index of refraction at low intensity, n_2 is the nonlinear refractive index and I is the optical irradiance. In order to describe the propagation of an intense electromagnetic wave through a thin isotropic nonlinear optical media, we considered the two circular components of polarization of the electric field $\mathbf{E}_+$ and $\mathbf{E}_-$ as:

$$\mathbf{E} = \mathbf{E}_+ + \mathbf{E}_- \tag{2}$$

then, the index of refraction for each component of polarization can be written as [10]:

$$n_\pm = n_0 + \frac{2\pi}{n_0}\left[A\left|E_\pm\right|^2 + (A+B)\left|E_\mp\right|^2\right] \tag{3}$$

where $A = \mathrm{Re}[6\chi^{(3)}_{1122}]$ and $B = \mathrm{Re}[6\chi^{(3)}_{1221}]$, are the components of the third-order nonlinear optical susceptibility, described by the tensor $\chi^{(3)}$. The real and the imaginary part of $\chi^{(3)}$ can be associated with the refractive and the absorptive nonlinearities, respectively. The components of $\chi^{(3)}$ are mathematically related by [10],

$$\chi^{(3)}_{1111} = \chi^{(3)}_{1122} + \chi^{(3)}_{1212} + \chi^{(3)}_{1221} \tag{4}$$

The nonlinear refractive index can originate from different physical mechanisms in the material itself; molecular orientation, electronic polarization, electrostriction or excited-state population are some examples among others phenomena that can generate an index nonlinearity. Nevertheless, the manifestation of each one of these

effects also depends on the beam wavelength, the energy fluence, and the pulse duration of the optical excitation.

For the case of the electrostriction effect, that is the manifestation of an elastic strain originated by an electric field, $\chi^{(3)}_{1111}$ can be characterized as [11],

$$\chi^{(3)}_{1111} = \frac{1}{\varepsilon_0}\frac{\gamma_e}{\upsilon_a^2}\frac{\partial\varepsilon}{\partial\rho} = \frac{\varepsilon_0}{27\,\upsilon_a^2\,\rho}\left(n_0^2+2\right)^2\left(n_0^2-1\right)^2 \tag{5}$$

with,

$$n_2 = \frac{12\pi^2}{n_0^2 c}10^7\chi^{(3)}_{1111} \tag{6}$$

here n_2 is the nonlinear refractive index in [cm^2/W], $\chi^{(3)}_{1111}$ in [esu], ε_0 represents the permittivity of the vacuum, υ_a represents the acoustic speed through the media, ρ represents the density of mass and γ_e is the electrostriction coefficient.

From Eqs. (5), (6) it is clear that the speed of propagation υ_a of a mechanical wave induced by an optical excitation is a function of n_2. Therefore, in a metallic nanocomposite where n_2 is strongly dependent on the participation of the LSPR, a modulation of the mechanical properties could be obtained by the influence of optical excitations.

3. Experiment

3.1. Au:TiO_2 sample synthesis

The Au NPs embedded in TiO_2 thin solid films were obtained using a sol–gel method as it has been previously described [12]. The Au NPs were synthesized with and without the participation of platinum in order to shift their optical absorptive band associated with their LSPR. The platinum doped sample was prepared with a Pt/Au molar ratio of 0.1. An atomic force microscope (AFM) (dimension 3100, nanoscope IV) with a lateral resolution of 1 nm and a vertical resolution of 0.1 nm was used to measure the size and density of the Au NPs in the resulting samples considering the vibrational spectra of the studied systems [13].

3.2. Linear optical response

The linear absorption spectra of the thin solid films were acquired with a Perkin Elmer XLS UV–visible spectrophotometer. Measurements of the refractive index under a low level of irradiation were performed by detecting the Brewster angle at 532 nm wavelength.

3.3. Nonlinear optical response

The third-order nonlinear optical properties of the samples were investigated using a vectorial two-wave mixing experiment [5]. A 532 nm wavelength and 1 ns duration

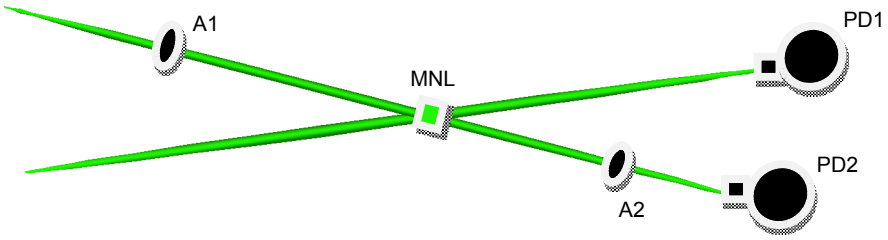

Fig. 1. Experimental setup. MNL – the sample, A1, A2 – polarizers, PD1, PD2 – photodetectors.

pulse was provided by the second harmonic of a Nd-YAG laser source. Figure 1 illustrates the experimental setup. MNL represents the sample, A1, A2 are polarizers, and PD1, PD2 are photodetectors with integrated filters. Pump and probe beams, with linear polarizations making an angle of 45°, are in simultaneous propagation in the same region of interaction of the studied sample. A single pulse with maximum energy of 80 mJ was employed as a pump beam, while a pulse with 10 nJ of energy was used as a probe beam. The diameter of the beam waist for the pump beam in the sample was measured to be 6 mm and for the probe beam it was 1 mm. The polarized irradiances of the transmitted beams in the two-wave interaction were measured in different cases of polarization of the incident beams making an angle ϕ between their planes of polarization. The axes of transmission of the analyzers A1 and A2 were aligned in order to detect the orthogonal components of the polarization of the waves.

3.4. Estimation of the Young's modulus by electrostriction measurements

Equations (5) and (6) together with the measured value of n_2 lead us to evaluate the change in the speed of the induced mechanical waves through the samples with a nanosecond beam; then the correspondent Young's modulus M was calculated by [14],

$$M = v_a^2 \rho \tag{7}$$

Furthermore, the strain ε allows to describe the deformation of a solid sample due to an applied stress; it can be calculated by,

$$\varepsilon = \frac{\sigma}{M} \tag{8}$$

here M is the Young's modulus and σ represents the average normal stress, that is,

$$\sigma = \frac{F}{A} \tag{9}$$

with F representing the applied force and A is the area.

4. Results and discussion

The thickness of the selected resulting films was close to 250 nm and the refractive index was about $n = 2.6$ for the 532 nm wavelength. The optical absorbance spectra are presented in Fig. 2. One can clearly observe the absorbing bands associated with the LSPR of the NPs with a blue shift of the resonance from 600 nm to approximately 450 nm resulting from the platinum doping in the preparation of the sample.

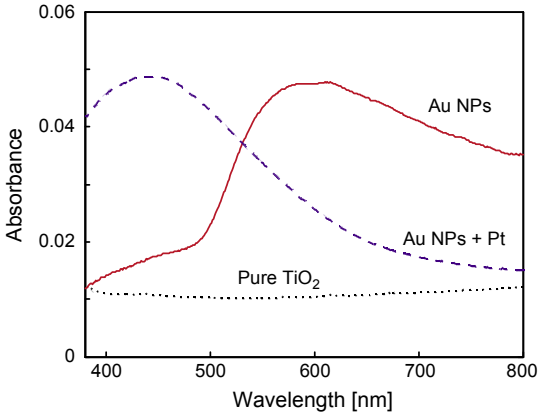

Fig. 2. Optical absorbance in the studied samples.

In order to measure the Au NPs size and density in the resulting films, a statistical cumulative analysis of several AFM micrographs of the samples with Au NPs was undertaken. The data was recorded in standard tapping mode. Figure 3 shows a representative AFM image obtained in the analysis of the thin film samples. The results of the statistical analysis showed that important differences in the particle size were obtained through the different films. In the samples without platinum, the average size of the Au NPs was approximately 87 nm, while for the platinum doped samples

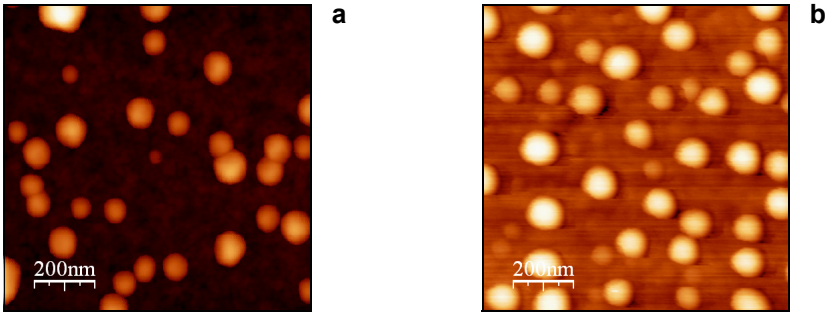

Fig. 3. Typical AFM micrograph of the selected thin films samples with embedded Au NPs: in a TiO_2 matrix (**a**) and in a Pt-doped TiO_2 matrix (**b**).

the result was approximately 110 nm. The particle density in both cases results in about 1.55×10^{9} cm^{-2} ± 20%.

To perform the nonlinear optical experiments, our measurement system was previously calibrated using carbon disulfide (CS_2) with a thickness of D = 1 mm, as a nonlinear medium with a well-known third-order nonlinear susceptibility of $|\chi^{(3)}| = 1.9\times10^{-12}$ esu [10].

We use the expressions for the amplitudes of the transmitted fields derived elsewhere [5]:

$$E_{1\pm}(z) = \left[E^0_{1\pm}J_0\left(\Psi^{(1)}_{\pm}\right) + (iE^0_{2\pm} - iE^0_{3\pm})J_1\left(\Psi^{(1)}_{\pm}\right) - E^0_{4\pm}J_4\left(\Psi^{(1)}_{\pm}\right)\right]\times$$
$$\times \exp\left(-i\Psi^{(0)}_{\pm} - \frac{\alpha(I)z}{2}\right) \tag{10}$$

$$E_{2\pm}(z) = \left[E^0_{2\pm}J_0\left(\Psi^{(1)}_{\pm}\right) + (iE^0_{4\pm} - iE^0_{1\pm})J_1\left(\Psi^{(1)}_{\pm}\right) - E^0_{3\pm}J_2\left(\Psi^{(1)}_{\pm}\right)\right]\times$$
$$\times \exp\left(-i\Psi^{(0)}_{\pm} - \frac{\alpha(I)z}{2}\right) \tag{11}$$

where $E_{1\pm}(z)$ and $E_{2\pm}(z)$ are the complex amplitudes of the circular components of the transmitted waves beams; $E_{3\pm}(z)$ and $E_{4\pm}(z)$ are the amplitudes of the self-diffracted waves, while $E^0_{1\pm}$, $E^0_{2\pm}$, $E^0_{3\pm}$, and $E^0_{4\pm}$ are the amplitudes of the incident and self-diffracted waves at the surface of the sample; $\alpha(I) = \alpha_0 + \beta I$ is the irradiance dependent absorption coefficient, where α_0 and β are the linear and two-photon absorption coefficients, respectively; I is the total irradiance of the incident beams; $J_m(\Psi^{(1)}_{\pm})$ stands for the Bessel function of order m, z is the thickness of the nonlinear media, and

$$\Psi^{(0)}_{\pm} = \frac{4\pi^2 z}{n_0\lambda}\left[\left(A + \frac{n_0\beta}{2\pi}\right)\sum_{j=1}^{4}\left|E_{j\pm}\right|^2 + \left(A + B + \frac{n_0\beta}{2\pi}\right)\sum_{j=1}^{4}\left|E_{j\mp}\right|^2\right] \tag{12}$$

$$\Psi^{(1)}_{\pm} = \frac{4\pi^2 z}{n_0\lambda}\left[\left(A + \frac{n_0\beta}{2\pi}\right)\sum_{j=1}^{3}\sum_{k=2}^{4}E_{j\pm}E^*_{k\pm} + \left(A + B + \frac{n_0\beta}{2\pi}\right)\sum_{j=1}^{3}\sum_{k=2}^{4}E_{j\mp}E^*_{k\mp}\right] \tag{13}$$

are the nonlinear phase changes. Here the optical wavelength is represented by λ.

By comparing numerical simulations of Eqs. (10)–(13) with the data obtained from the transmitted irradiances in the thin film samples, we obtained the nonlinear optical parameters. Figure 4 shows the experimental transmittance of the probe beam with the best fitting of the numerical simulations. These results are consistent with the reported values obtained in a similar sample with a different temporal regime with picosecond pulses [12].

The estimated n_2 and β parameters are presented in Table 1.

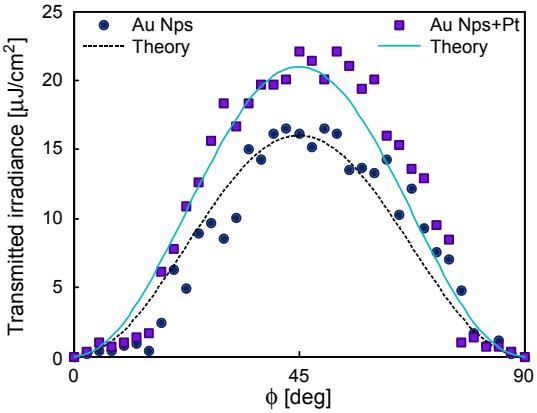

Fig. 4. Nonlinear optical results.

T a b l e 1. Nonlinear optical parameters.

Sample	β [m/W]	n_2 [m^2/W]	$\lvert\chi^{(3)}\rvert$ [esu]
Au NPs + TiO_2	1.0×10^{-9}	7×10^{-15}	1.17×10^{-8}
Au NPs + TiO_2 + Pt	1.1×10^{-9}	2×10^{-14}	3.34×10^{-8}

As a comparative result, we measured the nonlinear refraction for a pure TiO_2 sample and then we found that $n_2 = 7\times10^{-17}$ m^2/W. This last result is in a good agreement with the nonlinear optical response previously reported for samples prepared with different processing routes [15].

Since the thermo-optical effect can generate a density expansion that is an opposite modification in the nonlinear refractive index with respect to an electrostrictive force, we studied the change in the refractive index by thermo-optical response of the sample excited by a nanosecond pulse. We locate the sample in the arm of a Michelson interferometer operating at a 532 nm wavelength. From our results there was not an observable change in the position of the fringe patterns for an expanded single nanosecond pulse with 80 mJ detected by a CCD camera; however we were able to obtain a noticeable variation in the interferometric response after 6 seconds of exposition of a semiconductor laser at 445 nm wavelength and 1.25 W. Experimental results of a representative measurement are shown in Fig. 5. The white squares plotted on Fig. 5 were put on the same position of the pattern to clearly observe the fringe displacements.

Regarding the displacement in an interference fringe pattern observed in Fig. 5, it can be estimated a change in the refractive index by [16],

$$2\Delta n = m\lambda \tag{14}$$

where $2\Delta n$ represents the modification in the optical path in an arm of the interferometer, Δn is the change in the refractive index and m is related to the number of

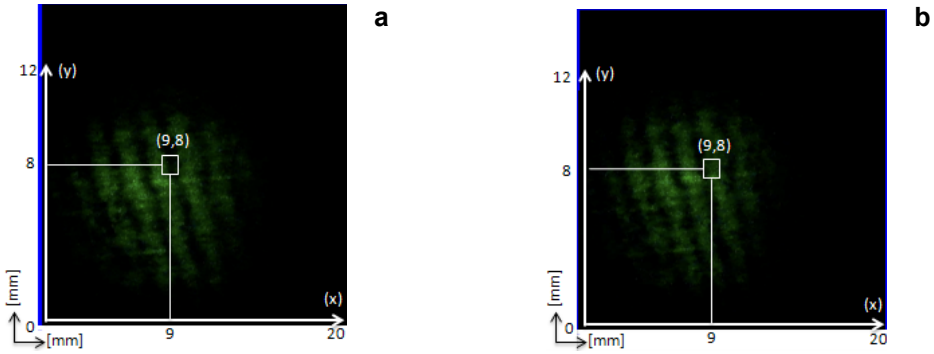

Fig. 5. Modification in the interferometric fringe pattern when the TiO_2 sample with embedded Au NPs is in steady state of temperature (**a**), irradiated during 6 s by a 1.25 W at 445 nm (**b**).

fringes. Our estimation of Δn for the thermal nonlinearity excited by the 445 nm beam is about 1×10^{-5}.

We calculated the heat-transference generated by optical irradiation in propagation through the samples by using [17],

$$\frac{\partial T}{\partial t} = \frac{\partial}{\partial z}\left[\frac{\kappa}{\rho C}\frac{\partial T}{\partial z}\right] + \frac{\alpha}{\rho C} I(t, z) \tag{15}$$

here T is the temperature, which is a function of the depth $z = 250$ nm, the thermal conductivity $\kappa = 3.34$ W/m·K, the density $\rho = 0.01908$ mol/cm^3, the heat capacity $C = 298.15$ J/mol·K, the time of irradiation $t = 6$ s, the linear absorption coefficient $\alpha = 65$ m^{-1} and I is the optical intensity. The results are presented in Fig. 6.

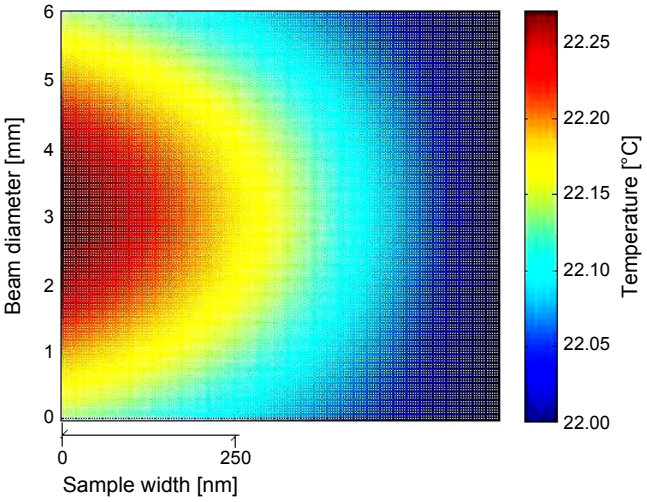

Fig. 6. Numerical heat transference originated by a Gaussian beam in propagation through a TiO_2 sample with embedded Au NPs.

We assume that the participation of the LSPR in the nonlinear optical properties can accelerate the propagation speed of mechanical waves. We calculated the change in the Young's modulus of our sample by using Eq. (7). It is possible to observe an important decrease in the Young's modulus of the sample, after the inclusion of platinum, by comparing the maximum and minimum points plotted in Fig. 7.

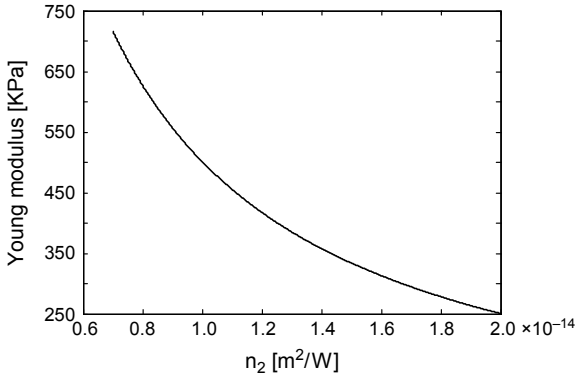

Fig. 7. Change in the Young's modulus *vs*. nonlinear refractive index.

As it can be seen from Fig. 7, a strong nonlinear modification of the Young's modulus can be achieved by the shift of the LSPR in the TiO_2 containing Au NPs and platinum. The participation of the LSPR seems to be responsible for the enhancement in the nonlinearity of index [18–20] and therefore also it ought to be responsible for the change in the Young's modulus parameter. Apparently, the simultaneous propagation of optical and mechanical waves can potentially exhibit functional applications where it is mandatory to adjust or manipulate the mechanical properties in opto-mechanical systems [21].

It can be considered that from the modification of the optical properties in a nonlinear interaction also a change of the features of the mechanical waves can be derived [22]. Thus, in order to confirm the participation of an electrostriction effect dependent on irradiance without an important contribution from a thermal nonlinearity, a reduction of the beam diameter of the probe beam at the two-wave interaction was performed under a similar condition of single-pulse irradiance of the pump irradiation, then, there was observed a complete fading of the modulation in the polarization of the probe after its propagation through the sample. This case corresponds to the reduction of a strong inhomogenous profile of irradiation capable to generate the electrostriction [23].

Our conclusions about the change in the mechanical properties were confirmed by a nanoindenter NHT from CSM Instruments with a maximum load of 20 mN and a Berkovich diamond tip that shows a change from 941 to 727 MPa after the Pt doping of the TiO_2 sample with Au NPs. However, we used Eqs. (8) and (9) to calculate the variation in the induced strain that can originate from an average normal stress applied with a force of 20 mN, generated by the maximum irradiance induced in the studied samples. Experimental results shown in Fig. 8 showed that the mechanical

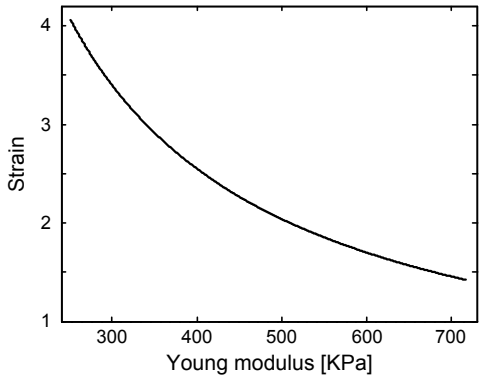

Fig. 8. Strain *vs*. Young's modulus.

measurements generate irreversible changes in the sample with shape deformations in more than twice the size of the film thickness; nevertheless nonlinear optical measurements allow the evaluation of mechanical parameters without perturbing the mechanical properties of the sample.

We can consider the possibility to modulate the strain in thin solid films by means of a laser system to adequate the mechanical properties of particular samples. Sensors or actuators in mechanical systems can be designed using this procedure.

5. Conclusions

Within this work, a modification of nonlinear optical properties and Young's modulus in a TiO_2 thin film with Au NPs was obtained by Pt doping. The nonlinear optical properties of the samples were compared by detecting the electrostriction effect induced by nanosecond pulses. Important differences in the nonlinear optical refraction and in the Young's modulus modification of the samples were achieved by the resulting shift of the LSPR of the NPs. Potential applications for tuning the optical and mechanical properties of nanodevices are contemplated.

Acknowledgements – We kindly acknowledge the financial support from Instituto Politécnico Nacional, from CIMAV, from Instituto de Ciencia y Tecnología del DF and from Consejo Nacional de Ciencia y Tecnología. The authors are also thankful to the Central Microscopy facilities at the Centro de Nanociencias y MicroNanotecnologías del IPN.

References

[1] CHIH-CHING HUANG, ZUSING YANG, HUAN-TSUNG CHANG, *Synthesis of dumbbell-shaped Au–Ag core–shell nanorods by seed-mediated growth under alkaline conditions*, Langmuir **20**(15), 2004, pp. 6089–6092.

[2] OVECHKO V., SCHUR O., MYGASHKO V., *Optical properties of the porous glass composite material*, Optica Applicata **38**(1), 2008, pp. 75–82.

[3] GANG WANG, YU ZHANG, YIPING CUI, MUYUN DUAN, MI LIU, *Study on the non-linear refraction of silver nanoparticles with aggregation effect*, Optics Communications **249**(1–3), 2005, pp. 311–317.

[4] WHITNEY A.V., ELAM J.W., SHENGLI ZOU, ZINOVEV A.V., STAIR P.C., SCHATZ G.C., VAN DUYNE R.P., *Localized surface plasmon resonance nanosensor: a high-resolution distance-dependence study using atomic layer deposition*, Journal of Physical Chemistry B **109**(43), 2005, pp. 20522–20528.

[5] TREJO-VALDEZ M., TORRES-MARTÍNEZ R., PERÉA-LÓPEZ N., SANTIAGO-JACINTO P., TORRES-TORRES C., *Contribution of the two-photon absorption to the third order nonlinearity of Au nanoparticles embedded in TiO_2 films and in ethanol suspension*, Journal of Physical Chemistry C **114**(22), 2010, pp. 10108–10113.

[6] STEPANOV A.L., *Applications of ion implantation for modification of TiO_2: a review*, Reviews on Advanced Materials Science **30**(2), 2012, pp. 150–165.

[7] JINXIA XU, XIANGHENG XIAO, STEPANOV A.L., FEN REN, WEI WU, GUANGXU CAI, SHAOFENG ZHANG, ZHIGAO DAI, FEI MEI, CHANGZHONG JIANG, *Efficiency enhancements in Ag nanoparticles–SiO_2–TiO_2 sandwiched structure via plasmonic effect-enhanced light capturing*, Nanoscale Research Letters **8**(1), 2013, article 73.

[8] MUÑOZ-CÉSAR J. C., TORRES-TORRES C., MORENO-VALENZUELA J., TORRES-TORRES D., URRIOLAGOITIA-SOSA G., TREJO-VALDEZ M., *Identification of inhomogenous optical absorptive response by chaotic photonic signals in Au nanoparticles*, Measurement Science and Technology **24**(3), 2013, article 035603.

[9] GUISBIERS G., KAZAN M., VAN OVERSCHELDE O., WAUTELET M., PEREIRA S., *Mechanical and thermal properties of metallic and semiconductive nanostructures*, Journal of Physical Chemistry C **112**(11), 2008, pp. 4097–4103.

[10] BOYD R., *Nonlinear Optics*, Academic Press, San Diego ,1992.

[11] SUTHERLAND R., *Handbook of Nonlinear Optics*, Marcel Dekker, New York, 1996.

[12] CAMPOS-LÓPEZ J.P., TORRES-TORRES C., TREJO-VALDEZ M., TORRES-TORRES D., URRIOLAGOITIA--SOSA G., HERNÁNDEZ-GÓMEZ L.H., URRIOLAGOITIA-CALDERÓN G., *Optical absorptive response of platinum doped TiO_2 transparent thin films with Au nanoparticles*, Materials Science in Semiconductor Processing **15**(14), 2012, pp. 421–427.

[13] ESPINOZA F., MUNOZ J., TORRES D., TORRES R., SCHNEIDER A., *Atomic force microscopy cantilever simulation by finite element methods for quantitative atomic force acoustic microscopy measurements*, Journal of Materials Research **21**, 2006, pp. 3072–3079.

[14] ALBRECHT T.R., AKAMINE S., CARVER T.E., QUATE C.F., *Microfabrication of cantilever styli for atomic force microscopy*, Journal of Vacuum Science and Technology A **8**(4), 1990, pp. 3386–3396.

[15] ILIOPOULOS K., KALOGERAKIS G., VERNARDOU D., KATSARAKIS N., KOUDOUMAS E., COURIS S., *Nonlinear optical response of titanium oxide nanostructured thin films*, Thin Solid Films **518**(4), 2009, pp. 1174–1176.

[16] HECHT E., *Optica*, Calypso, San Francisco, 2002.

[17] VON ALLMEN M., BLATTER A., *Laser-Beam Interaction with Materials*, Springer, Berlin, 1995.

[18] ANIJA M., JINTO THOMAS, NAVINDER SINGH, SREEKUMARAN NAIR A., RENJIS T. TOM, PRADEEP T., REJI PHILIP, *Nonlinear light transmission through oxide-protected Au and Ag nanoparticles: an investigation in the nanosecond domain*, Chemical Physics Letters **380**(1–2), 2003, pp. 223–229.

[19] LIU LI, SU XIONG-RUI, *Enhanced optical nonlinear absorption of graded Au–TiO_2 composite films*, Chinese Physics B **17**(6), 2008, pp. 2170–2174.

[20] MINJOUNG KYOUNG, MINYUNG LEE, *Z-scan studies on the third-order optical nonlinearity of Au nanoparticles embedded in TiO_2*, Bulletin of the Korean Chemical Society **21**(1), 2000, pp. 26–28.

[21] LONG HUA, YANG GUANG, CHEN AI-PING, LI YU-HUA, LU PEI-XIANG, *Multilayer Au/TiO_2 composite films with ultrafast third-order nonlinear optical properties*, Chinese Physics Letters **25**(11), 2008, pp. 4135–4138.

[22] GRINDLAY J., *Electrostriction*, Physics Review **160**(3), 1967, pp. 698–701.

[23] SHEN Y.R., *Electrostriction optical Kerr effect and self-focusing of laser beams*, Physics Letter **20**(4), 1966, pp. 378–380.

Received December 19, 2012
in revised form March 22, 2013